

Motivation

- Previous studies over the Pacific Northwest (PNW) (e.g., IMPROVE-2; Lin et al. 2009, etc.) showed an overprediction of windward precipitation and snow aloft for bulk micro parameterizations (BMPs).
- BMPs encounter large uncertainties to riming and other ice characteristics (habit, size distribution, density, etc.) (Colle et al. 2017, Naeger et al., 2017).

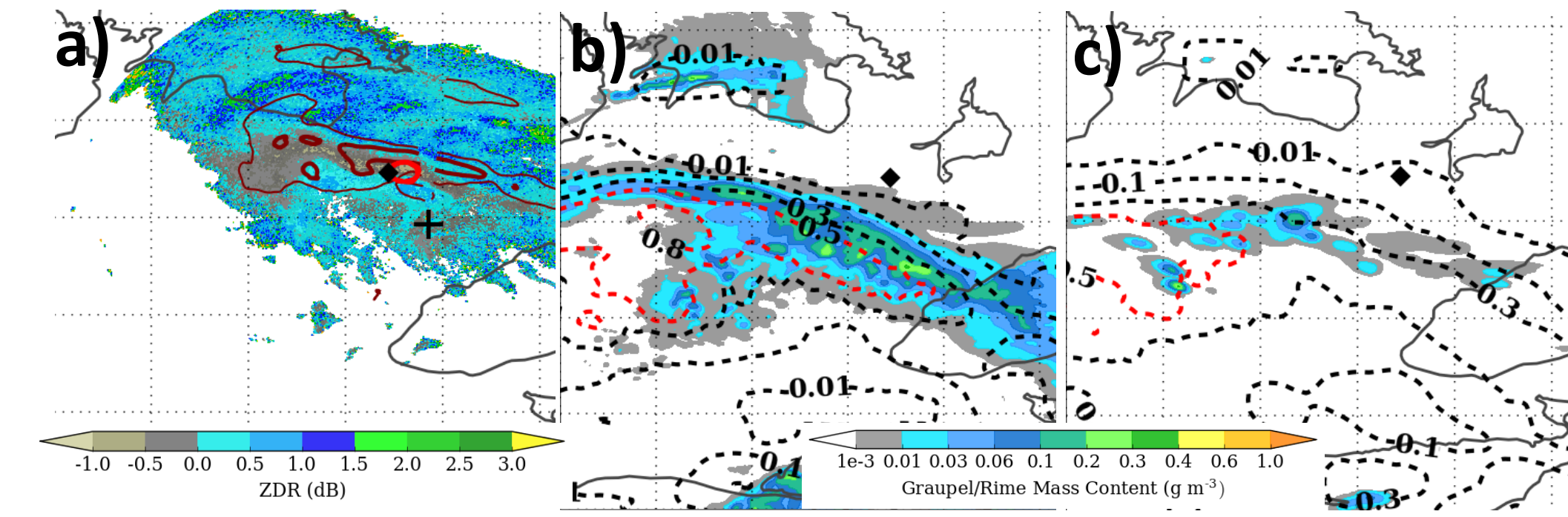


Figure 1 (top). Observed vs modeled snow (red values and black contours) and cloud water (blue values and grey shades)

Figure 2 (left). (a) King City radar observations of ZDR and dBZ (maroon, thin contour 18 dBZ, thick contour 24 dBZ) during snowfall event on 18 February 2012 during GCPEX campaign. (b) Graupel/rime mass content and cloud liquid water path (contoured at 0.01, 0.1, and 0.3 g m⁻² in black and 0.5 and 0.8 g m⁻² in red) from the (b) Predicted Particle Properties (P3) and (c) Morrison (MORR) BMP schemes.

NPOL/NEXRAD and Soundings

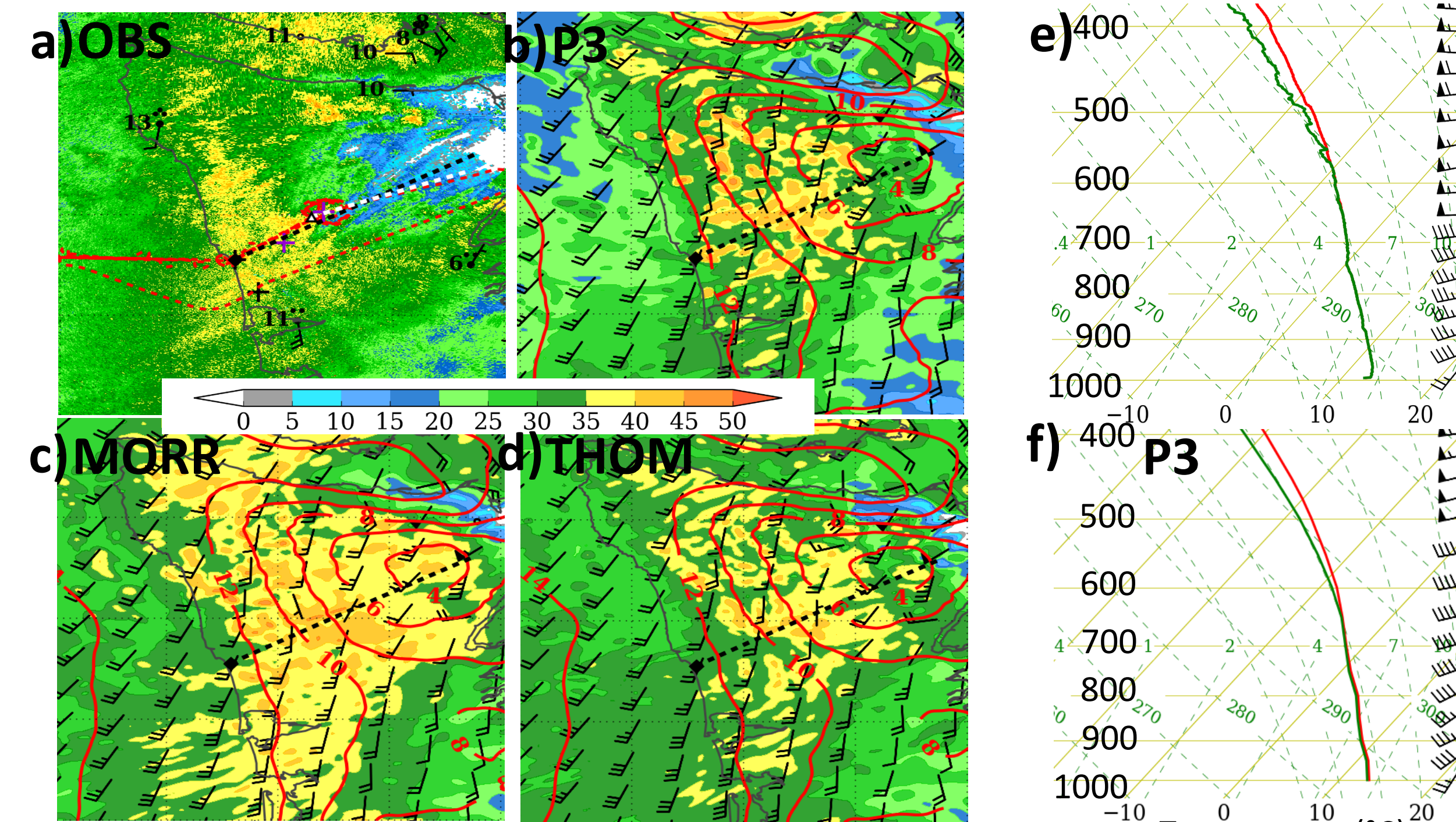


Figure 4. (a) Observed radar reflectivity (0.5° scan) from NPOL and WSR-88Ds (KRTX, KLGX, KATX sites) at (a) 01 UTC Nov 13, with station observations also shown. (b) P3 reflectivity, 10-m winds, and 2-m temperatures from same time. (c-d) Same as (b), except for (c) MORR and (d) THOM. (e) Colorado State University (CSU) rawinsonde at NPOL site on 13 Nov 03 UTC. (f) Modeled sounding from P3 at same time and location.

- Enhancement of precipitation along windward slopes in both observations and model.
- All WRF schemes show similar precipitation structures prior to ~06 UTC 13 Nov.
- WRF also shows good comparison to rawinsondes during this period.

UND citation and Precip Ground Sites

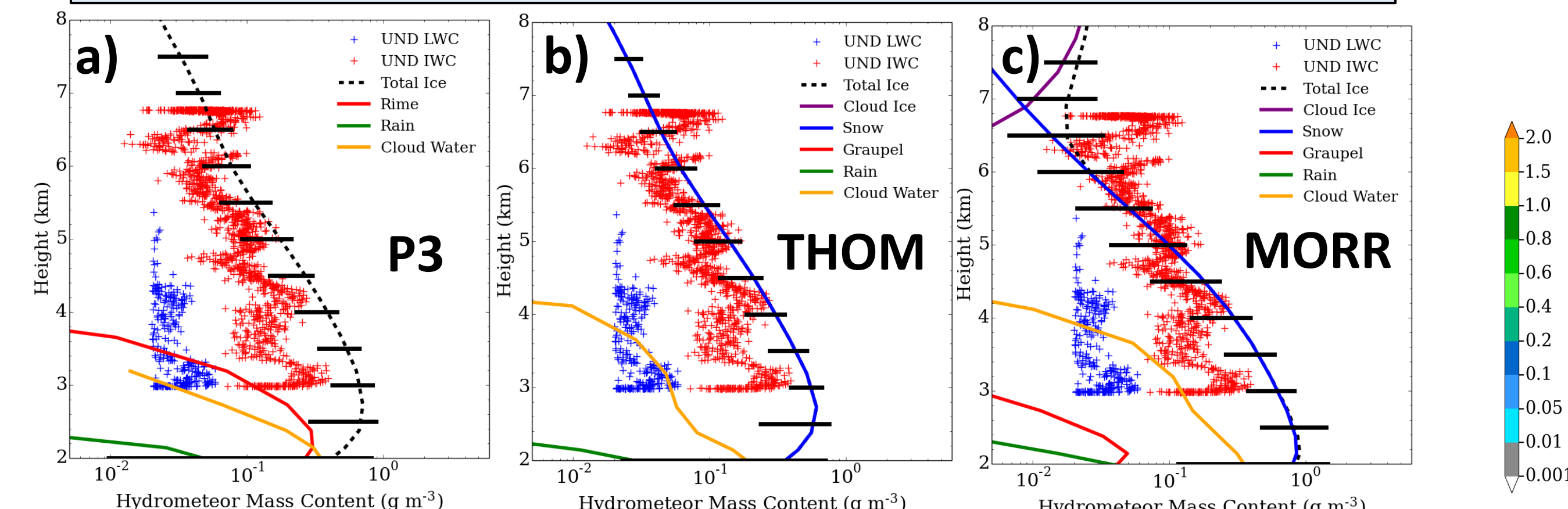


Figure 7. (a) UND citation measurements of hydrometeor content during spiral ascent at ~2000 UTC 12 Nov along with mass contents from P3 at same time. (b) THOM and (c) MORR mass contents.

- Significant ice water contents of > 0.2 g m⁻³ observed below 4 km.
- Increasing trend in total ice content in P3 and THOM compares reasonably well with citation, albeit schemes show overall larger values.
- Sharp decrease in total ice near 2 km in P3 and THOM associated with melting layer, with melting layer in MORR much less apparent.

Satellite Observations

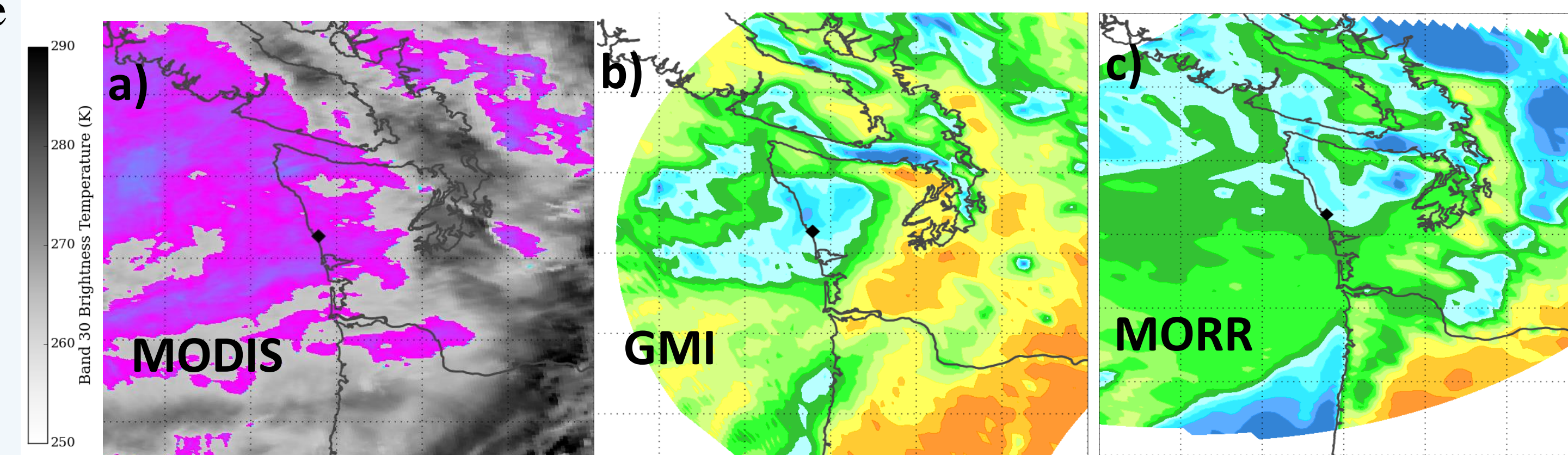


Figure 9. (a) Aqua MODIS 11 μm brightness temperatures (BTs) at ~2200 UTC 12 Nov with pixels < 263 K shaded. (b) GMI 89 GHz (horizontal) BTs near same time. (c) Synthetic GMI 89 GHz BTs calculated from MORR scheme.

12-13 Nov 2015 Event

NPOL/DOW RHI scans

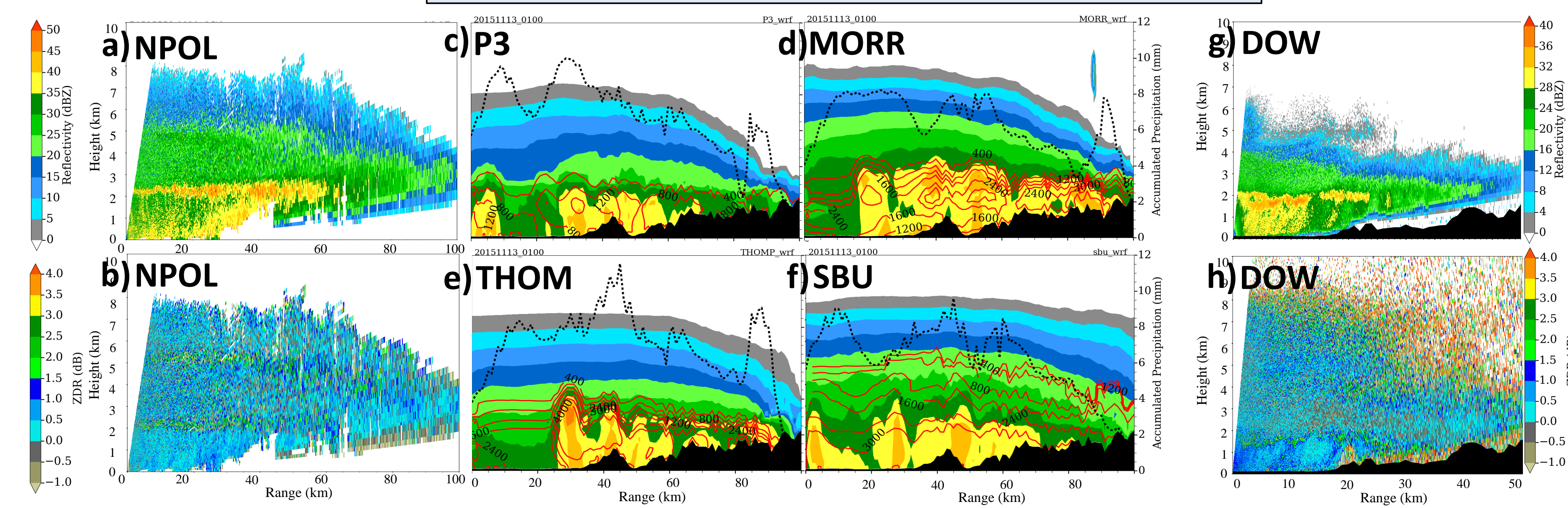


Figure 5. (a) Observed radar reflectivity and (b) differential reflectivity (ZDR) along NPOL RHI scan at ~01 UTC 14 Nov, and (c) P3 reflectivity (shaded), rain number concentration (red contours), and 1-h precip totals (black contours) for same time and cross section. (d-f) Same as (c), but for MORR, THOM, and SBU schemes, respectively. (g) DOW reflectivity and ZDR earlier in the event (~22 UTC 12 Nov).

- NPOL reveals deep cloud nearly 8 km in height with an ice growth region likely causing the enhanced dBZ and ZDR at ~5 km. Strong dBZ below a distinct melting layer at ~2 km.
- P3 predicts most realistic precip structure with areas of enhanced dBZ below ~2 km, other schemes predict some enhanced dBZ extending to 4 km in height.
- P3 predicts lower rain number concentration than other schemes due to larger raindrop sizes.
- Areas of ZDR > 0.5 in NPOL and DOW suggest presence of some larger raindrops.

WRF Hydrometeor/Microphysical Processes

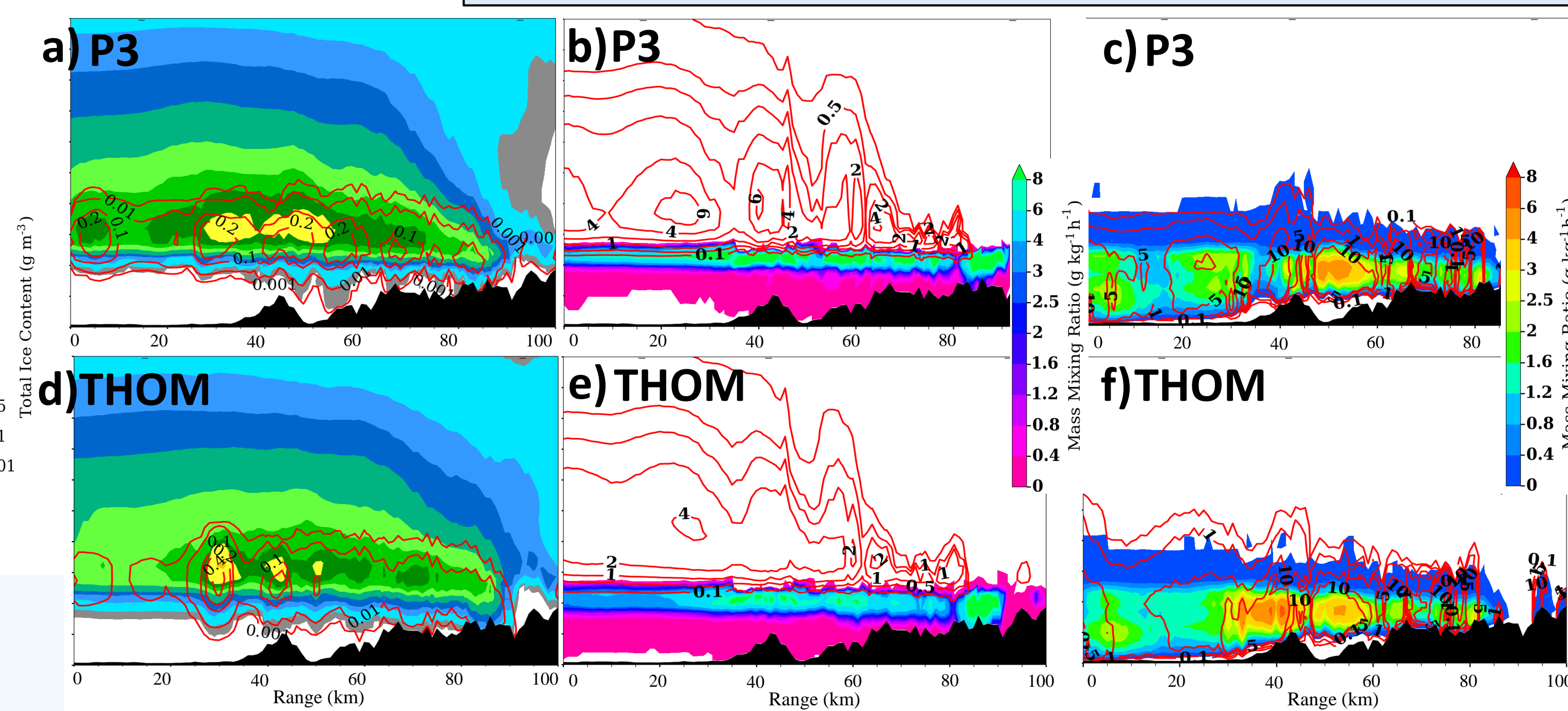


Figure 6. (a) P3 total ice (shaded) and rimed content (contoured) at 01 UTC 13 Nov. (b) Deposition (contoured) and cold rain mixing ratios (shaded), along with (c) cloud condensation (contoured) and warm rain mixing ratios (shaded). (d-f) Same as (a-c), but for THOM.

- P3 predicts larger total ice content and rime/graupel content than THOM.
- Stronger depositional growth in P3 leading to enhanced melting layer and cold rain production.
- THOM predicts weaker melting layer and stronger warm rain processes than P3.

Summary and Future Work

P3 predicts stronger deposition and ice particle growth than other schemes, which leads to the efficient sedimentation of ice particles into a well-defined melting layer. These stronger cold rain processes in P3 influence smaller droplet concentrations and larger rain accumulations that better compare to observations. We will continue our validation work using the other OLYMPEX cases, while also conducting LES simulations down to ~100 m grid spacing to help further realize deficiencies in the BMP schemes. Simulations of past field campaign events will also be utilized to conduct a broader validation of the BMPs.

* This work is supported by grant NNX16AD81G.

Model Setup and Configuration

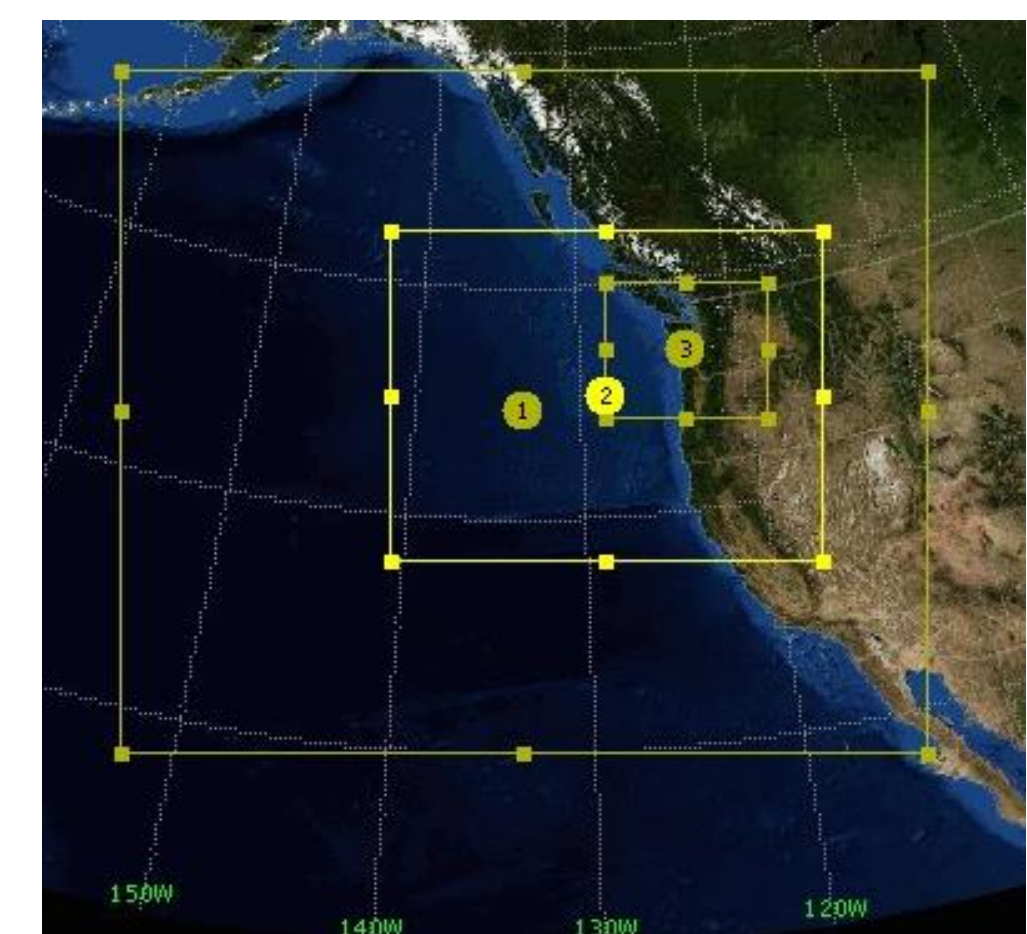


Figure 3. WRF model grid configuration

BMP schemes

- Thompson (THOM); ~2D ice, ice size distribution from Field et al. (2005), variable riming efficiency.
 - Morrison (MORR); 2-moment, spherical ice/snow.
 - Stony Brook (SBU); ~2D ice/snow, combines snow/graupel into one category, degree of riming estimated and variations in snow density.
 - P3; Four prognostic mixing ratio variables predict the bulk particle properties of a single ice-phase. Adverts ice/rime properties.
- To aid in validating/refining BMPs, we also run HUJI (Hebrew University) bin scheme; calculates size distributions based on 33 mass bins for hydrometeor types.

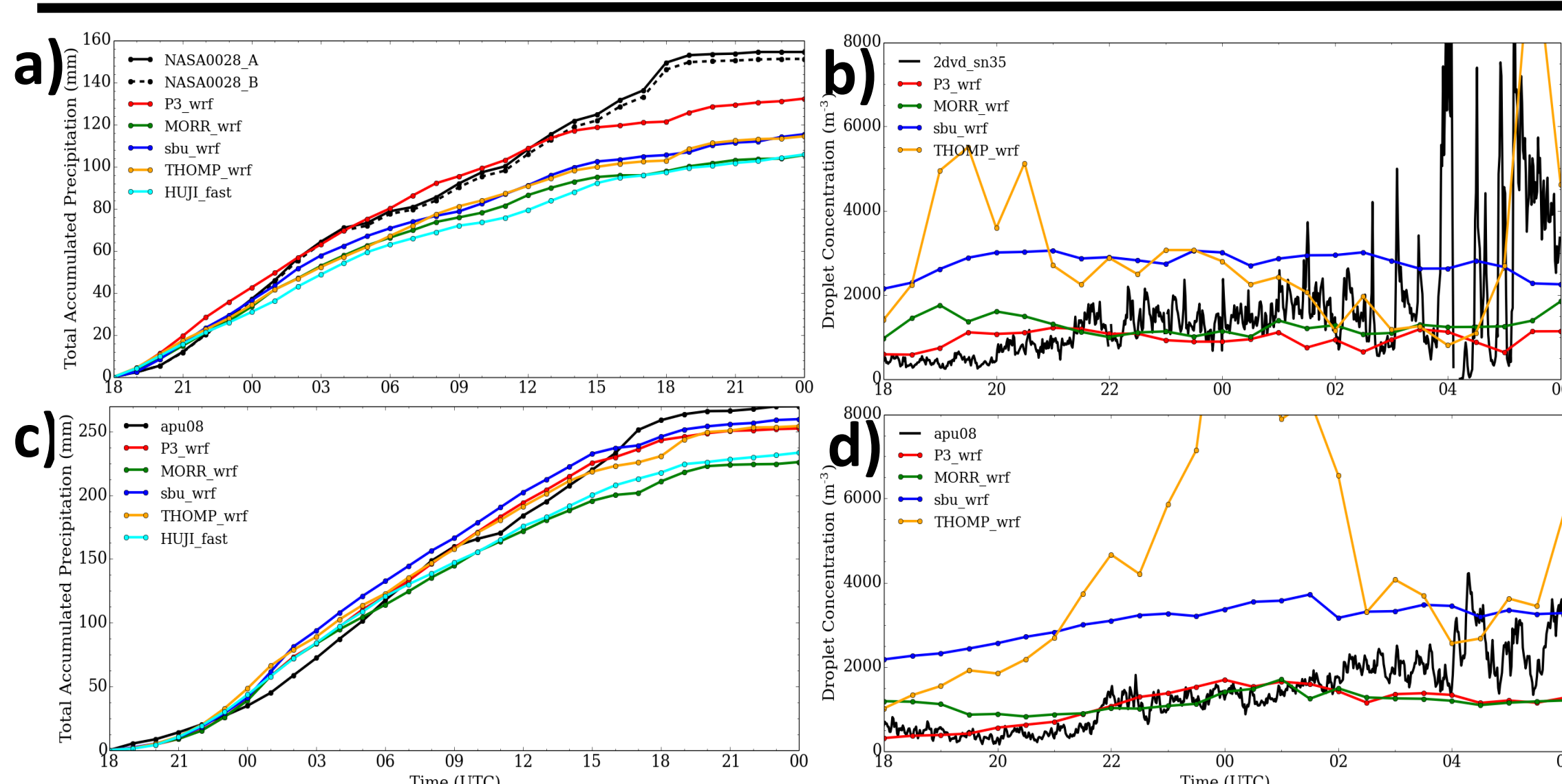


Figure 8. (a) Total precip (NASA gauge) and (b) droplet concentrations (2dv4) at Fishery compared to WRF schemes. (c-d) Same as (a-b) except APU measurements at Bishop/CRN.

- P3 shows closer comparison to total precip at Fishery site due to more dominant cold rain processes.
- Lower precip totals in MORR from much weaker melting layer.
- Unrealistically large droplet concentrations in THOM suggests too strong of warm rain processes.